Journal of Marine Science and Technology

Volume 18 | Issue 4 Article 6

AN ANALYTICAL SOLUTION TO THE MODIFIED MILD-SLOPE EQUATION FOR WAVES PROPAGATING AROUND A CIRCULAR CONICAL ISLAND

Sung-Shan Hsiao
Department of Harbor and River Engineering, National Taiwan Ocean University, Keelung, Taiwan, R.O.C.

Chun-Ming Chang
Department of Harbor and River Engineering, National Taiwan Ocean University, Keelung, Taiwan, R.O.C.

Chih-Chung Wen
Department of Safety, Health and Environmental Engineering, Hungkuang University, Taichung county, Taiwan, R.O.C, wen1558@sunrise.hk.edu.tw

Journal of Marine Science and Technology, Vol. 18, No. 4, pp. 520-529 (2010)

AN ANALYTICAL SOLUTION TO THE MODIFIED MILD-SLOPE EQUATION FOR WAVES PROPAGATING AROUND A CIRCULAR CONICAL ISLAND

Sung-Shan Hsiao*, Chun-Ming Chang*, and Chih-Chung Wen**

Key words: modified mild-slope equation, conical island, analytical solution, Hunt's direction solution of dispersion relation.

ABSTRACT

There are many analytical solutions to the mild-slope equation that employ Hunt's direct solution of linear dispersion [7] to solve wave-scattering problems involving varying quiescent depths. The advantage of Hunt's direct solution of linear dispersion is that it can extend the range of applicability of the mild-slope equation from long-wave to deep-wave conditions. However, because the bottom curvature and slope-squared terms are neglected, the mild-slope equation cannot preserve mass conservation. In this investigation, we derived an analytic solution of the modified mild-slope equation for a conical island by adopting Hunt's direct solution of linear dispersion to be applicable to intermediate water depth waves. We studied three differently slopes of conical islands in this paper. The relative difference between the present solution, including extended terms, and the conventional mild-slope equation proposed by Liu and Lin [11] was also estimated. The relative difference is insignificant in the long waves cases of the conical island; the maximal difference is just 0.4%.

In contrast with the long waves conditions, the relative difference in the case of intermediate water waves is as high as 8.7% in $T = 120$ sec with a bottom slope of 1:3. Our analytical procedure shows that the 3rd Hunt's approximation can perform as well as the conventional mild-slope equation proposed by Liu and Lin [11], which involves a 5th approximation. Finally, the relative difference between the present solution and the conventional mild-slope equation proposed by Liu and Lin [11] increases as the azimuth of the conical island decreases.

Paper submitted 07/13/09; accepted 08/07/09. Author for correspondence: Chih-Chung Wen (e-mail: wen1558@sunrise.hk.edu.tw).
**Department of Harbor and River Engineering, National Taiwan Ocean University, Keelung, Taiwan, R.O.C.*
***Department of Safety, Health and Environmental Engineering, Hungkuang University, Taichung county, Taiwan, R.O.C.*

I. INTRODUCTION

Accurate prediction of water wave transformation over an irregular topography on which structures may be situated is important to engineers who plan, design, construct, and maintain coastal facilities. Phenomena such as refraction, diffraction, reflection, shoaling, and wave breaking take place when water waves propagate from deep to shallow water. Generally, numerical, experimental and analytical methods are adopted to predict wave transformation. Because the physical model lacks any approximations, testing experimental data against numerical results is the preferred method of study. However, experimental data is expensive and time-consuming to obtain. Furthermore, poor experimental technique leads to erroneous data. Numerical models are based on approximation. Numerical models can be tested against analytical solutions, as the accuracy of an analytical solution is limited only by the assumptions employed in deriving the solution. Although analytical solutions are often available only for certain special cases under idealized assumptions, they have the advantages of being quick, simple and accurate. It is also easier to use analytical solutions to evaluate the influence of specific forcing or boundary conditions on the problem.

Analytical solutions are generally only obtainable for simple bottom topographies and particular types of waves. MacCamy and Fuchs [13] proposed a solution to the Helmholtz equation for a cylindrical island standing in an open sea with constant depth. However, constant water depth is an ideal case. To describe a wave propagating over complex bottom topography, the mild-slope equation (MSE), proposed by Berkhoff [1], is an appropriate way of approximating the refraction and diffraction of linearized surface waves for water of varying quiescent depth. The MSE is widely applied, not only in long-wave conditions but also in short-wave conditions. The mild-slope equation would reduces to the Helmholtz equation in short-wave conditions and becomes the linear shallow water equation in long-wave conditions. A frequently considered problem in analytical studies of water wave transformation is long-wave motion around a circular island mounted on an

axisymmetric shoal. Homma [5] proposed solutions to the linear shallow water equation for a circular cylindrical island mounted on a parabolic shoal. Zhang and Zhu [18] presented a series solution to the linear shallow water equation for water wave scattering by a conical island. Zhu and Zhang [19] proposed an analytical solution, in the form of a Fourier-cosine series, for long-wave scattering by a circular cylindrical island mounted on a conical shoal. Based on the linear shallow water equation, Yu and Zhang [17] published a form of the solutions for axisymmetric bottom geometries that can be described as a power of the radial distance. In addition, Suh *et al*. [16] presented an analytical solution for a long wave propagating over a parabolic pit, in which the water depth varies as the second power of the radial distance from the pit center.

However, the analytical solutions of the shallow water equation mentioned above are restricted to long-wave conditions. An analytical solution to MSE is very difficult to obtain, even though it is only a simple linear partial differential equation. The implicit wave dispersion relation on varying topography is the main barrier to obtaining the corresponding wave number. To overcome this difficulty, recently Liu *et al*. [12] employed Hunt's [7] Padé approximation to the linear dispersion relation to represent MSE in terms of a combination of Fourier series and Taylor series and proposed an analyticcal solution for the combined wave refraction and diffraction around a circular cylindrical island mounted on a parabolic shoal. Using this method, a series of related studies was published. Lin and Liu [11] proposed an analytical solution based on MSE for wave scattering and trapping of wave energy by a submerged truncated parabolic shoal. Similarly, Liu and Lin [11] presented an analytical solution for the combined refraction-diffraction of plane monochromatic waves by a circular cylinder mounted on a conical shoal in an otherwise open sea of constant depth. Jung and Suh [8] derived an analytical solution to MSE for a wave propagating over an axisymmetric pit, and extended the solution to the nearly vertical side slope trench. Furthermore, Jung *et al*. [10] attempted to derive an analytical solution for a wave propagating over a trench composed of a linear slope and an abrupt change of depth. The analytical results were compared with those of the hyperbolic MSE.

Booij [2] compared the numerical results from MSE with finite element model results for the reflection coefficients of monochromatic wave propagating over a planar slope and concluded that MSE is sufficiently accurate for bottom slope values below 1:3. However, many investigations [4, 6, 14, 15] have pointed out that the conventional MSE fails to produce adequate approximations for rapidly changing topographies or uneven seabed. The bottom curvature and slope-squared terms play an important role in uneven topography, especially in regions of intermediate water depth. To account for these terms Jung and Suh [9] presented an analytical solution to the modified mild-slope equation (MMSE) [3] for a long wave propagating over an axisymmetric pit. However, this analytical solution is restricted to long-wave conditions.

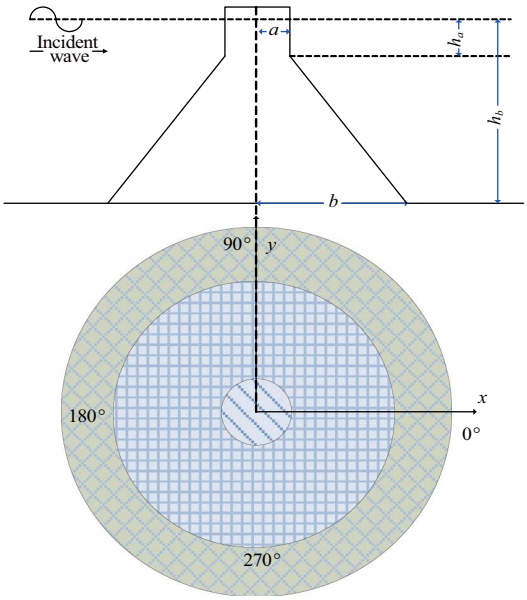

Fig. 1. Sketch of a circular cylindrical island mounted on an axisymmetric shoal.

Hunt's direct solution can extend MSE to the whole range from long wave to short wave. To the best of the author's knowledge, MMSE has never been solved analytically for intermediate water depth conditions. The principle difficulty in solving MMSE analytically comes from the fact that the bottom slope-squared term and bottom curvature term are very complex and hard to simplify. In this investigation, by adopting the linear wave dispersion relation from Hunt's direct solution and transforming the implicit *kh* (relative depth) into an explicit power series, we not only derive an analytical solution to MMSE for waves propagating around a circular cylinder mounted on an axisymmetric conical shoal in an otherwise open sea of constant depth, but also extend the solution to intermediate water depth conditions.

II. ANALYTICAL SOLUTION

Consider the scattering of simple harmonic waves by a circular cylindrical island mounted on a conical shoal (Fig. 1), where a, b, h_a, and h_b are the radius of the top cylinder, the radius of the toe of the bottom shoal, the water depth along the coastline, and the constant water depth outside the island, respectively. Let (x, y, z) be Cartesian coordinates, set up so that $z = 0$ corresponds to the quiescent free surface position of an incompressible fluid in irrotational motion. The origin is located at the center of the island on the quiescent free surface. The water elevation $\eta = \eta(x, y)$ satisfies the following MMSE [3]:

$$\nabla_h \cdot [CC_g \nabla_h \eta] + [k^2 CC_g + f_1(kh) g \nabla_h^2 h + f_2(kh) gk (\nabla_h h)^2] \eta = 0 \quad (1)$$

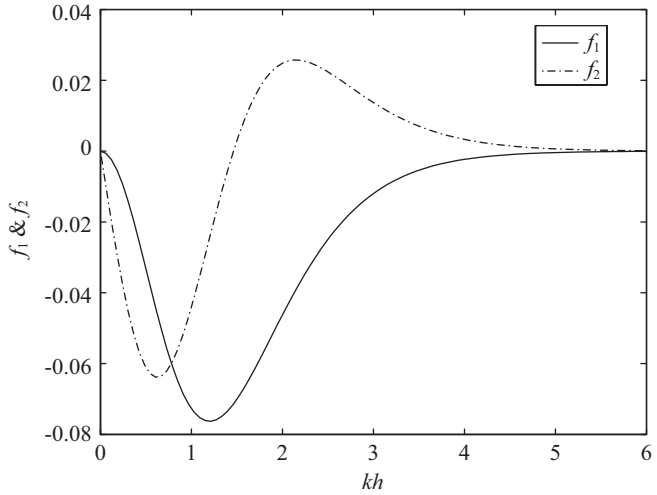

Fig. 2. Sketch of $f_1(kh)$ and $f_2(kh)$.

in which $\nabla_h( ) = (\partial( )/\partial x, \partial( )/\partial y)$ is the horizontal gradient operator; C is the phase velocity, C_g is the group velocity, g is the acceleration due to gravity, $h(x, y)$ is the water depth, $k(x, y)$ is the local wave number, and $(\nabla_h h)$ and $\nabla_h^2 h$ are the bottom slopes and bottom curvatures in the x and y directions, respectively.

$f_1(kh)$ and $f_2(kh)$ are both functions of kh, which take the form:

$$f_1(kh) = \frac{[-4kh\cosh kh + \sinh 3kh + \sinh kh + 8(kh)^2 \sinh kh]}{8\cosh^3 kh(2kh + \sinh 2kh)} - \frac{kh\tanh kh}{2\cosh^2 kh},$$

$$f_2(kh) = \frac{\operatorname{sech}^2 kh}{6[2kh + \sinh 2kh]^3}[8(kh)^4 + 16(kh)^3 \sinh 2kh - 9\sinh^2 2kh\cosh 2kh + 12kh(1 + 2\sinh^4 2kh)(2kh + \sinh 2kh)].$$

The coefficients of the curvature and slope-squared terms are plotted as functions of kh in Fig. 2. Both coefficients approach zero at in the shallow and deep water limits, and are most important in the range of intermediate water depth. If the last two terms in the brackets of (1) are removed, the governing equation is reduced to the conventional MSE.

We also have

$$C = \left(\frac{g\tanh kh}{k}\right)^{1/2}, C_g = \frac{C}{2}\left(1 + \frac{2kh}{\sinh 2kh}\right).$$

$k(x, y)$ is determined by the implicit dispersion relation

$$\omega^2 = gk\tanh(kh) \tag{2}$$

For convenience, we define the following dimensionless parameters:

$$C' = \frac{C}{\sqrt{ga}}, C_g' = \frac{C_g}{\sqrt{ga}}, \omega' = \sqrt{\frac{a}{g}}\omega, (x', y') = \frac{(x, y)}{a}, \eta' = \frac{\eta}{A},$$

$$h' = \frac{h}{a}, k' = ka.$$

As a consequence, the governing equation and dispersion relation become

$$\nabla'[C'C_g' \cdot \nabla'(\eta')] + [k'^2 \cdot C'C_g' + f_1(k'h') \cdot \nabla'^2(h') + f_2(k'h') \cdot k'(\nabla'h')^2]\eta' = 0 \tag{3}$$

and

$$\nu' \equiv K'\tanh(K'), \tag{4}$$

respectively, where $\nabla_h'( ) = (\partial( )/\partial x', \partial( )/\partial y')$, $\nu' = \omega'^2 h'$ and $\nu' = \omega'^2 h'$. Hereafter, all of the primes will be dropped for convenience. Since the topography is axisymmetric, polar coordinates defined by $x = r\cos\theta$ and $y = r\sin\theta$ will be used. In these coordinates, Eq. (3) may be written as

$$CC_g\frac{\partial^2\eta}{\partial r^2} + \frac{\partial(CC_g)}{\partial r}\frac{\partial\eta}{\partial r} + \frac{1}{r}CC_g\frac{\partial\eta}{\partial r} + \frac{1}{r^2}CC_g\frac{\partial^2\eta}{\partial\theta^2} + [\omega^2\frac{C_g}{C} + f_1 \cdot \nabla^2 h + f_2 \cdot k(\nabla h)^2]\eta = 0 \tag{5}$$

It was proven in Liu *et al*. [12] that the coefficients of (5), i.e., CC_g, C_g/C and $\partial(CC_g)/\partial r$ can be expressed as explicit functions:

$$CC_g = \frac{1}{2\omega^2}\frac{\nu}{K^2}\left(\nu - \nu^2 + K^2\right) \approx \frac{1}{2\omega^2}\frac{\left[P(\nu) + 1\right]\nu}{\nu P(\nu) + 1} \tag{6}$$

$$\frac{C_g}{C} = \frac{\nu - \nu^2 + K^2}{2\nu} \approx \frac{P(\nu) + 1}{2P(\nu)} \tag{7}$$

$$\frac{\partial\left(CC_g\right)}{\partial r} = \frac{1}{2}\frac{\left(K^2 - \nu^2\right)\left(K^2 - 3\nu^2 + 3\nu\right)}{K^2\left(K^2 - \nu^2 + \nu\right)}\frac{\partial h}{\partial r} \tag{8}$$

Therefore, Eq. (5) reads

$$\frac{1}{2\omega^2}\frac{\nu}{K^2}\left(\nu-\nu^2+K^2\right)\frac{\partial^2\eta}{\partial r^2}+\frac{1}{2}\frac{\left(K^2-\nu^2\right)\left(K^2-3\nu^2+3\nu\right)}{K^2\left(K^2-\nu^2+\nu\right)}\frac{\partial h}{\partial r}\frac{\partial \eta}{\partial r}$$

$$+\frac{1}{r}\frac{1}{2\omega^2}\frac{\nu}{K^2}\left(\nu-\nu^2+K^2\right)\frac{\partial\eta}{\partial r}+\frac{1}{r^2}\frac{1}{2\omega^2}\frac{\nu}{K^2}\left(\nu-\nu^2+K^2\right)\frac{\partial^2\eta}{\partial\theta^2}$$

$$[\omega^2\frac{\nu-\nu^2+K^2}{2\nu}+f_1\cdot\nabla^2 h+f_2\cdot k(\nabla h)^2]\eta=0 \tag{9}$$

The coefficients of (9) are still transcendental functions because of the implicit dispersion relation of (4). This makes an explicit solution to (9) impossible if no approximation of (4) is involved. This makes an explicit solution to (9), Hunt's Padé approximation direct solution of the implicit wave dispersion relation is employed as follows:

$$K=\sqrt{\nu^2+\frac{\nu}{1+\sum_{j=1}^{\infty}d_j\nu^j}}=\sqrt{\nu^2+\frac{\nu}{P(\nu)}} \tag{10}$$

The first six value of d_j in (10) can be found in Hunt's report published in 1979, and are: $d_1=\frac{2}{3}$, $d_2=\frac{16}{25}$, $d_3=\frac{152}{945}$, $d_4=\frac{128}{2025}$, $d_5=\frac{128}{6075}$ and $d_6=\frac{4736}{893025}$. For convenience, we denote $P_S(\nu)=\sum_{j=0}^{S}d_j\nu^j$, with d_0 = 1, and the corresponding direct solution will be called Hunt's s th-order approximate solution of the wave dispersion.

Although Hunt's approach can approximate the solution of liner dispersion relation as the order increase, the order of Hunt's direct solution should be truncated. Jung and Suh [8] pointed out that the relative error of Hunt's 4th order solution is less than 1%. In Fig. 3 we show the relative errors in calculation of phase speed for all values of ν. However, the Hunt's 4th order solution which is used later would make the analytical solution more complicated. Thus, the Hunt's 3rd order solution with 1.5% relative errors is employed in this paper. The coefficients of (9) can be simplified by substituting (10) into (6)-(8).

$$CC_g\approx\frac{1}{2\omega^2}\frac{\left[P(\nu)+1\right]\nu}{\nu P(\nu)+1} \tag{11}$$

$$\frac{C_g}{C}\approx\frac{P(\nu)+1}{2P(\nu)} \tag{12}$$

$$\frac{\partial\left(CC_g\right)}{\partial r}\approx\frac{3\left[P(\nu)+1\right]-2\left[\nu P(\nu)+1\right]}{2\left[P(\nu)+1\right]\left[\nu P(\nu)+1\right]}\frac{\partial h}{\partial r} \tag{13}$$

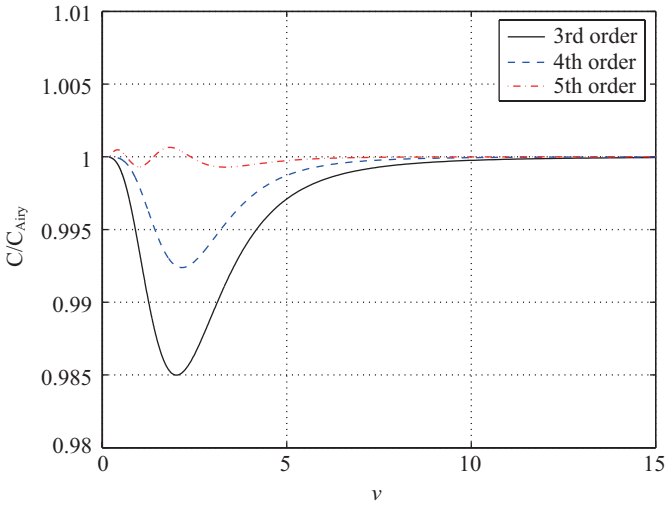

Fig. 3. Comparison of normalized phase speeds for different order of Hunt's solutions.

The bottom curvature and slope-squared terms also should be converted into explicit forms containing $P(\nu)$. The bottom slope-squared term of MMSE can be rewritten in the form:

$$f_2\cdot k(\nabla h)^2=f_2\cdot\frac{K}{h}(\nabla h)^2=f_2\cdot\frac{K}{\nu}\omega^2(\nabla h)^2 \tag{14}$$

Thus, the bottom slope-squared term becomes the following function:

$$f_2\cdot\frac{K}{\nu}\omega^2(\nabla h)^2=\frac{1}{12\nu P(\nu)(\nu P(\nu)+1)(P(\nu)+1)^3}$$
$$(\omega^2(6P(\nu)^2+2\nu^2P(\nu)-18P(\nu)^4\nu$$
$$+8\nu^2P(\nu)^2+12P(\nu)^4\nu^2+8\nu P(\nu)$$
$$-9P(\nu)^3+3P(\nu)+2\nu+6\nu^2P(\nu)^3))(\nabla h)^2 \tag{15}$$

Substituting the approximate solution (8) into (6), we have the following approximate form of MMSE:

$$6r^2\nu^2P(\nu)\left[P(\nu)+1\right]^4\frac{\partial^2\eta}{\partial r^2}+6\omega^2r^2\nu P(\nu)\left[P(\nu)+1\right]^2$$
$$\left[3P(\nu)-2\nu P(\nu)+1\right]\frac{\partial h}{\partial r}+6r\nu^2P(\nu)\left[P(\nu)+1\right]^4]\frac{\partial\eta}{\partial r}$$
$$+6\nu^2P(\nu)\left[P(\nu)+1\right]^4\frac{\partial^2\eta}{\partial\theta^2}+[6\nu r^2\omega^4\left[P(\nu)+1\right]^4$$
$$[\nu P(\nu)+1]+r^2\omega^4(\omega^2(6P(\nu)^2+2\nu^2P(\nu)-18P(\nu)^4\nu$$

$$+8\nu^2P(\nu)^2+12P(\nu)^4\nu^2+8\nu P(\nu)-9P(\nu)^3+3P(\nu)$$

$$+2\nu+6\nu^2P(\nu)^3))(\nabla h)^2]\eta=0 \tag{16}$$

In this paper, the surface-piercing topography consists of a vertical circular cylinder on top of a conical submerged shoal. As shown in Fig. 1, the water depth in the finite region with varying quiescent depth is given by

$$h(r)=\begin{cases}\dfrac{h_a}{a}r, & 1\le r\le r_b\\ \dfrac{h_b}{a}, & r_b<r\end{cases} \tag{17}$$

where $r_b = b/a$. By employing the method of separation of variables, the solution of (16) can be expressed as

$$\eta_1(r,\theta)=\sum_{m=0}^{\infty}R_m(r)\cos m\theta,\left(1\le r\le r_b,0\le\theta<2\pi\right) \tag{18}$$

in which the integer m corresponds to the m th angular modes and $R_m(r)$ is the corresponding coefficient, which varies in the r direction. Substituting (18) into (16), we obtain the following equation:

$$6r^2\nu^2P(\nu)\left[P(\nu)+1\right]^4\frac{\partial^2R_m(r)}{\partial r^2}+[6\omega^2r^2\nu P(\nu)\left[P(\nu)+1\right]^2$$

$$\left[3P(\nu)-2\nu P(\nu)+1\right]\frac{\partial h}{\partial r}+6r\nu^2P(\nu)\left[P(\nu)+1\right]^4]\frac{\partial R_m(r)}{\partial r}$$

$$+[-m^2\,6\nu^2P(\nu)\left[P(\nu)+1\right]^4+6\nu r^2\omega^4\left[P(\nu)+1\right]^4[\nu P(\nu)+1]$$

$$+r^2\omega^4(\omega^2(6P(\nu)^2+2\nu^2P(\nu)-18P(\nu)^4\nu+8\nu^2P(\nu)^2$$

$$+12P(\nu)^4\nu^2+8\nu P(\nu)-9P(\nu)^3+3P(\nu)+2\nu+6\nu^2P(\nu)^3))$$

$$(\nabla h)^2]R_m(r)=0 \tag{19}$$

for m = 0, 1, 2, …, ∞. By substituting $h=\dfrac{h_a}{a}r$ into (19) and noting that $\nu = \varepsilon r$, with $\varepsilon = \omega^2h_a/a$, we get the following equation:

$$6r^4\varepsilon^2P(\varepsilon r)\left[P(\varepsilon r)+1\right]^4\frac{\partial^2R_m(r)}{\partial r^2}+[6\omega^2r^3\varepsilon P(\varepsilon r)\left[P(\varepsilon r)+1\right]^2$$

$$\left[3P(\varepsilon r)-2\varepsilon rP(\varepsilon r)+1\right]\frac{h_a}{a}+6r^3\varepsilon^2P(\varepsilon r)\left[P(\varepsilon r)+1\right]^4]\frac{\partial R_m(r)}{\partial r}$$

$$+[-m^2\,6r^2\varepsilon^2P(\varepsilon r)\left[P(\varepsilon r)+1\right]^4+6\varepsilon r^3\omega^4\left[P(\varepsilon r)+1\right]^4$$

$$[\varepsilon rP(\varepsilon r)+1]+r^2\omega^4[\omega^2[6P(\varepsilon r)^2+2\varepsilon^2r^2P(\varepsilon r)-18P(\varepsilon r)^4\varepsilon r$$

$$+8\varepsilon^2r^2P(\varepsilon r)^2+12P(\varepsilon r)^4\varepsilon^2r^2+8\varepsilon rP(\varepsilon r)-9P(\varepsilon r)^3+3P(\varepsilon r)$$

$$+2\varepsilon r+6\varepsilon^2r^2P(\varepsilon r)^3]](\frac{h_a}{a})^2]R_m(r)=0 \tag{20}$$

The zero-flux boundary condition along the coastline at r = 1 is equivalent to

$$\left.\frac{dR_m(r)}{dr}\right|_{r=1}=0, \tag{21}$$

for m = 0, 1, 2, …, ∞. Following the procedure proposed by Liu *et al*. [12], we expand $R_m(r)$ as a Taylor series around the point r = 1, which is an ordinary point of (19). The following mappings

$$t=\frac{1}{r},\ \bar{R}_m(t)=R_m\left(\frac{1}{t}\right) \tag{22}$$

are employed, and (19) then becomes

$$A(t)\frac{d^2\bar{R}_m(t)}{dt^2}+B(t)\frac{d\bar{R}_m(t)}{dt}+\left[C(t)-m^2D(t)\right]\bar{R}_m(t)=0 \tag{23}$$

for m = 0, 1, 2, …, ∞, where

$$A(t)=6\varepsilon^2t^4Q(t)\left(Q(t)+t^3\right)^4$$

$$B(t)=6\varepsilon^2t^3Q(t)^2\left(Q(t)+t^3\right)^2\left(Q(t)-t^3+2\varepsilon t^2\right)$$

$$C(t)=\varepsilon(24\omega^4\varepsilon t^3Q(t)^4+24\omega^4t^{13}Q(t)+24\omega^4t^7Q(t)^3$$

$$+6\omega^4\varepsilon t^{12}Q(t)+24\omega^4\varepsilon t^9Q(t)^2+6\omega^4\varepsilon Q(t)^5$$

$$+36\omega^4\varepsilon t^6Q(t)^3+36\omega^4t^{10}Q(t)^2+6\omega^4t^{16}+6\omega^4t^4Q(t)^4$$

$$+8\varepsilon^2t^{13}Q(t)+6\varepsilon^2t^6Q(t)^3+8\varepsilon^3t^9Q(t)^2+3\varepsilon t^{14}Q(t)$$

$$-18\varepsilon^2t^4Q(t)^4+2\varepsilon^2t^{16}+6\varepsilon t^{11}Q(t)^2-9\varepsilon t^8Q(t)^3$$

$$+2\varepsilon^3t^{12}Q(t)+12\varepsilon^2t^3Q(t)^4)$$

$$D(t)=6\varepsilon^2t^2Q(t)\left(Q(t)+t^3\right)^2,$$

with $Q(t)=t^3\overline{P}\left(\frac{1}{t}\right)=t^3+\frac{2}{3}\varepsilon t^2+\frac{16}{45}\varepsilon^2 t+\frac{152}{945}\varepsilon^3$. Because of the mapping of (22), the varying depth in the inner region is mapped onto $1/r_b \le t \le 1$. Fortunately, the expansion point r = 1, even it has been mapped into $t=1$, is still an ordinary point of (23). The general solution of (23) imposed by the boundary condition (21) can be expressed in a Taylor series as follows:

$$\bar{R}_m(t)=\alpha_m\sum_{s=0}^{\infty}\frac{a_{m,s}}{s!}(t-1)^s \tag{24}$$

where

$$a_{m,0}=1$$

$$a_{m,1}=0$$

$$a_{m,0}=-[C(1)-m^2D(1)]/A(1)$$

$$a_{m,s}=\frac{-1}{A(1)}\left\{\sum_{p=1}^{s-2}\binom{s-2}{p}A^{(p)}(1)a_{m,s-p}+\sum_{p=0}^{s-2}\binom{s-2}{p}B^{(p)}(1)a_{m,s-p-1}\right.$$

$$\left.+\sum_{p=0}^{s-2}\binom{s-2}{p}[C^{(p)}(1)-m^2D^{(p)}(1)]a_{m,s-p-2}\right\},\qquad s=3,4,... \tag{25}$$

in which $A^{(p)}(1)$, $B^{(p)}(1)$, $C^{(p)}(1)$ and $D^{(p)}(1)$ denote the p th-order derivatives of $A(t)$, $B(t)$, $C(t)$ and $D(t)$ at the expansion point t = 1, respectively. Since $A(t)$, $B(t)$, $C(t)$ and $D(t)$ are all polynomials, and so their derivatives can be obtained analytically without any numerical error. We now investigate the convergence of (23). The convergence of the Frobenius series is dependent upon the behavior of the first variable coefficient in (23), i.e., $6\varepsilon^2t^4Q(t)(Q(t)+t^3)$. Besides the singularity at t = 0, there may exist singularities in $6\varepsilon^2t^4Q(t)(Q(t)+t^3)$. The singular points are calculated from the roots of $A(t)$ = 0. It is easy to obtain all of the roots of $A(t)$ = 0:

$$t_1=-0.5510977183\varepsilon,$$

$$t_{2,3,4,5}=-0.3965099140\varepsilon,$$

$$t_{6,7}=(-0.05778447414\pm 0.5371468390i)\varepsilon,$$

$$t_{8,9,10,11,12,13,14,15}=(0.03158829036\pm 0.4492550483i)\varepsilon,$$

$$t_{16,17,18,19}=0,$$

where $i=\sqrt{-1}$. Obviously, if $\bar{R}(t)$ is expanded around the ordinary point t = 1, the series and its derivatives converge for all complex t within the disk $|t-1|\le\rho$, where ρ is the distance from t = 1 to the nearest singularity. In Fig. 4, we plot

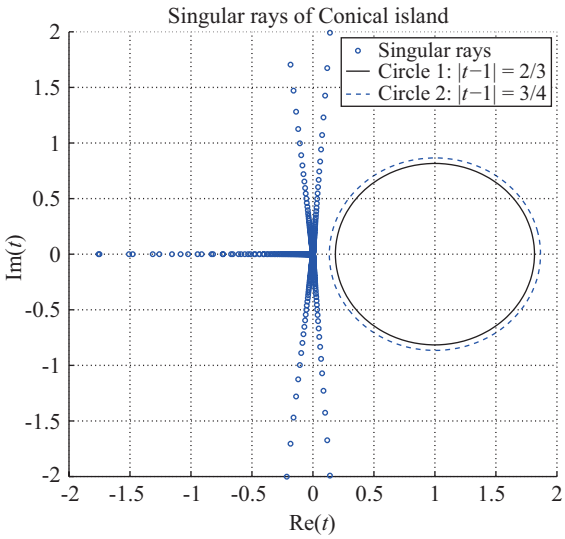

Fig. 4. Singular rays of (23), where circle 1 and 2 represent islands with r_b = 3 and r_b = 4, respectively.

the four rays consisting of the singular points in the complex plane, while the incident wave periods vary from short to long wave. We follow the previous work conducted by Liu and Lin [11]. The cases r_b = 3 (circle 1) and r_b = 4 (circle 2) are chosen to make sure that the present analytical solution converges uniformly in the inner varying depth regions. The smallest convergent radius is from the expansion point (t = 1 in our study) to the nearest singular point, and it is obvious in Fig. 4 that circle 1 and circle 2 do not encompass the singular rays. This means that if $r_b \le 4$, then the Taylor series in (24) converges uniformly for arbitrary incident waves.

From (18) and (24), the water surface in the various depth regions can be expressed as

$$\eta_1(r,\theta)=\sum_{m=0}^{\infty}R_m(r)\cos m\theta=\sum_{m=0}^{\infty}\bar{R}_m(t)\cos m\theta$$

$$=\sum_{m=0}^{\infty}\alpha_m\sum_{s=0}^{\infty}\frac{a_{m,s}}{s!}(t-1)^s\cos m\theta \tag{26}$$

In the constant water depth region, the well-known analytical solution was derived by MacCamy and Fuchs [13], and is given by

$$\eta_2(r,\theta)=\sum_{m=0}^{\infty}\left[i^m\beta_mJ_m(k_br)+\gamma_mH_m^{(1)}(k_br)\right]\cos m\theta, \tag{27}$$
$$(r_b<r,0\le\theta<2\pi)$$

where $J_m(k_br)$ is the Bessel function of the first kind of order m, $H_m^{(1)}(k_br)$ is the Hankel function of the first kind of order m, k_b is the wave number of constant depth h_b/a, and the Jacobi symbols are defined as

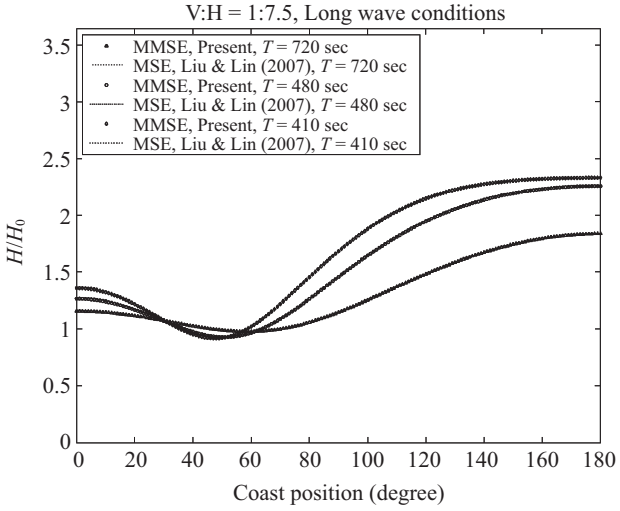

Fig. 5. The dimensionless wave height around the conical island (long wave, 1:7.5).

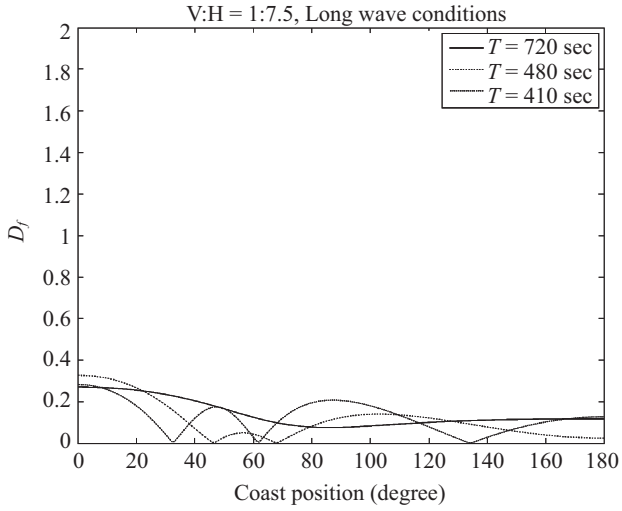

Fig. 6. The D_f around the conical island (long wave, 1:7.5).

$$\beta_m = \begin{cases} 1, & m = 0 \\ 2, & m \geq 1 \end{cases}. \tag{28}$$

Finally, the coefficient α_m must be determined by applying the following dynamic and kinematics matching conditions at $r = r_b$.

$$\eta_1\Big|_{r=r_b} = \eta_2\Big|_{r=r_b} \quad , \quad \frac{\partial \eta_1}{\partial r}\bigg|_{r=r_b} = \frac{\partial \eta_2}{\partial r}\bigg|_{r=r_b} , \tag{29}$$

respectively. By using this matching process and the Wronskian identity $J_m(k_b r_b) H_m^{(1)'}(k_b r_b) - J_m'(k_b r_b) H_m^{(1)}(k_b r_b) = 2i/\pi k_b r_b$, the coefficients α_m and γ_m can be found to be

$$\alpha_m = \frac{2 i^{m+1} \beta_m}{\pi r_b \left[\tilde{R}_m(r_b) H_m^{(1)'}(k_b r_b) - \tilde{R}_m'(r_b) H_m^{(1)}(k_b r_b) \right]}$$

$$\gamma_m = \frac{i^m \beta_m \left[k_b \tilde{R}_m(r_b) J_m'(k_b r_b) - \tilde{R}_m'(r_b) J_m(k_b r_b) \right]}{\tilde{R}_m'(r_b) H_m^{(1)}(k_b r_b) - k_b \tilde{R}_m(r_b) H_m^{(1)'}(k_b r_b)}$$

where $\tilde{R}_m(r) = \sum_{s=0}^{\infty} \frac{a_{m,s}}{s!} (t-1)^s$. Note that a prime denotes a derivative. Thus, we can compute the water surface elevation throughout the whole domain by substituting the coefficients back into (26) and (27).

III. RESULTS AND DISCUSSION

The analytical solution for η involves an infinite series, which must be properly truncated in practical calculation. Thus, we must find an appropriate integer m that is large enough that the infinite series of (26) is approximated to a desired accuracy. In this paper, we calculated the series by summing terms until the results satisfied the following condition: $\frac{a_{m,S}}{S!}(t-1)^S \Big/ \sum_{s=0}^{S} \frac{a_{m,s}}{s!}(t-1)^s < 10^{-6}$. To understand the effect of the bottom slope-squared term in shallow water and intermediate water depth conditions, we calculated the solutions for various values of $k_b h_b$. Furthermore, different slopes are also calculated to address the effect of the slope. This was done by changing the radius of the conical island, b. The values used for the radius are 30000 m, 23335 m and 18001 m and the corresponding slopes (vertical: horizontal) are 1:7.5, 1:5 and 1:3, respectively. In addition, to study the difference between the present analytical solution and the analytical solution proposed by Liu and Lin [11], we define a difference index based on the relative error. The difference index is expressed as $D_f = \frac{|\eta_{MMSE} - \eta_{MSE}|}{\eta_{MMSE}} \cdot 100\%$, where η_{MSE} is the η obtained by the mild-slope equation and η_{MMSE} the modified mile-slope equation.

1. Slope 1:7.5

First, the analytical solutions are discussed for long wave and intermediate water depth waves conditions, respectively. We set the wave periods to 720, 480, 410,360, 240 and 120 seconds, and the corresponding values of $k_b h_b$ are 0.1772, 0.2676, 0.3146, 0.36, 0.5549 and1.2990, respectively. The comparisons between our analytical solutions and the analytical solutions of Liu and Lin [11] under the conditions of long wave are shown in Figs. 5-8. It can be seen in Fig. 5 that the present analytical solution, based on Hunt's 3rd-order solution for the dispersion and Liu and Lin's method [11] is evidently excellent. Figure 6 shows that the relative difference

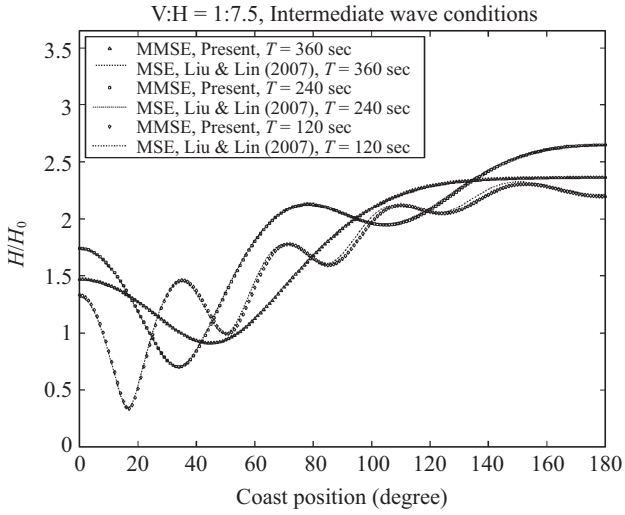

Fig. 7. The dimensionless wave height around the conical island (intermediate water wave, 1:7.5).

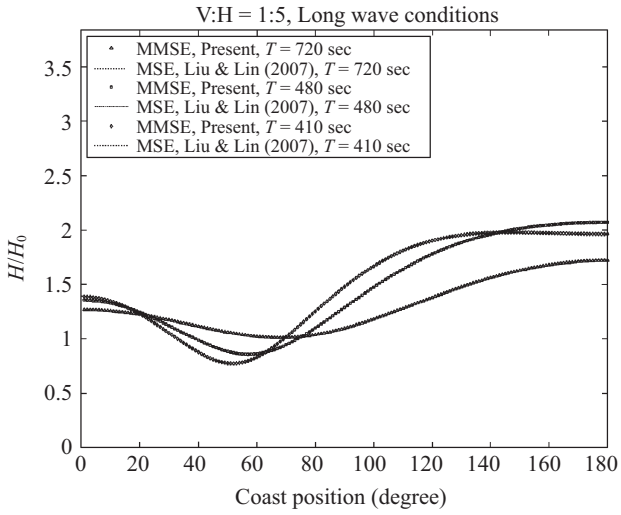

Fig. 9. The dimensionless wave height around the conical island (long wave, 1: 5).

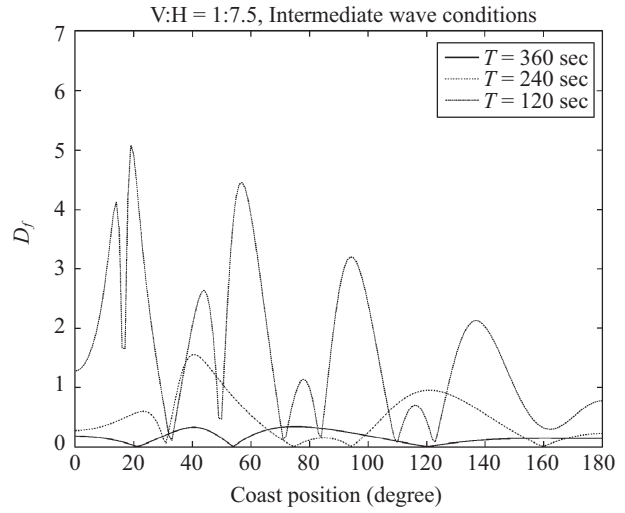

Fig. 8. The D_f around the conical island (intermediate water wave, 1:7.5).

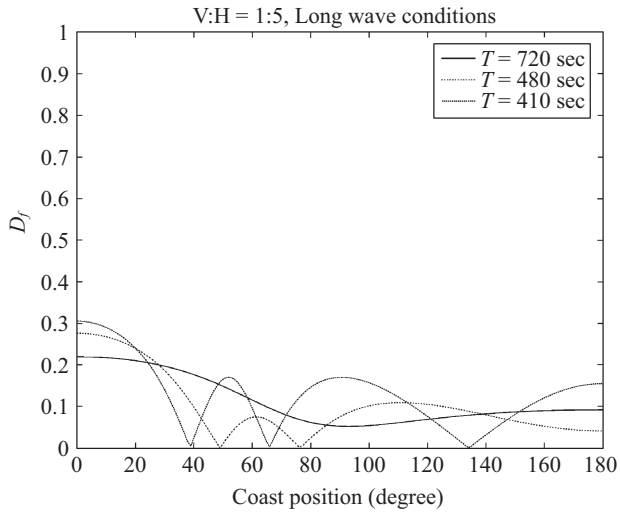

Fig. 10. The D_f around the conical island (long wave, 1:5).

between the present analytical solution to MMSE and the solution to MSE proposed by Liu and Lin [11]. The maximal D_f at a slope of 1:7.5 is less than 0.35%, which occurs at 0° with the wave period T = 480 sec.

For the intermediate water waves, the wave periods are set to 360, 240 and 120 sec. Figure 7 represents the dimensionless wave height around the conical island and shows good agreement with the maximal D_f of 5% (Fig. 8).

2. Slope 1:5

To gain some insight into the effect of the slope, cases with steeper slopes are examined. Figures 9-12 show the waves propagate around a conical island with slope 1:5, while the wave conditions are the same as the previous case of slope 1:3. Figure 9 shows the results for the long wave conditions, and Fig. 10 shows the maximal D_f in long wave conditions, which is about 0.3%. Comparisons of the dimensionless wave heights of intermediate water depth waves around the conical island between the present solutions and Liu and Lin's [11] solutions are shown in Fig. 11. This figure shows slight discrepancies between present MMSE solutions and those of MSE derived by Liu and Lin [11]. The relative differences in these cases are plotted in Fig. 12, and the maximal D_f, which is less than 4% , occurs at 20° with a wave period of T = 120 sec.

3. Slope 1:3

Finally, the waves for the steepest bottom slope, a slope of 1:3, is calculated with the previous incident wave periods. The results are displayed in Figs.13-16. Figure 13 shows the excellent results for long wave conditions. Figure 14 shows the maximal D_f is about 0.25% for long wave conditions. This is because that the bottom extended terms are insignificant in

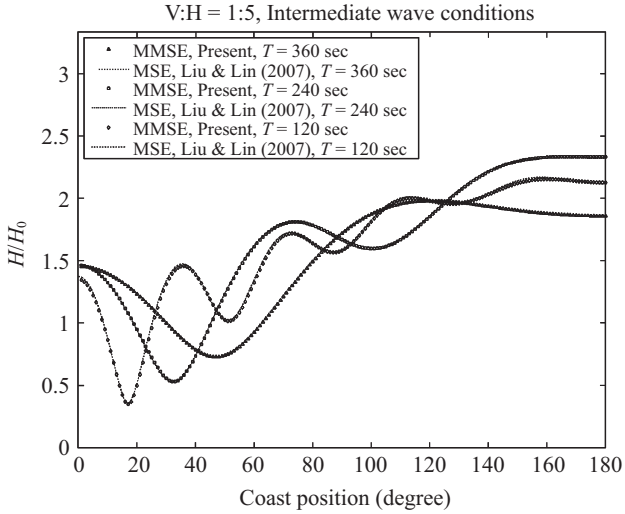

Fig. 11. The dimensionless wave height around the conical island (intermediate water wave, 1:5).

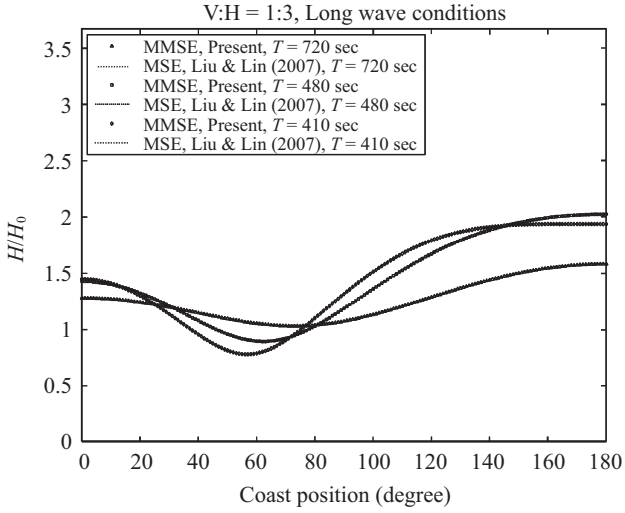

Fig. 13. The dimensionless wave height around the conical island (long wave, 1:3).

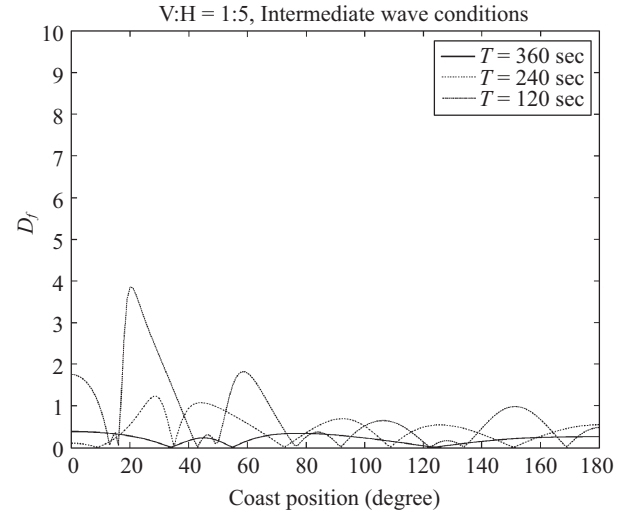

Fig. 12. The D_f around the conical island (intermediate water wave, 1:5).

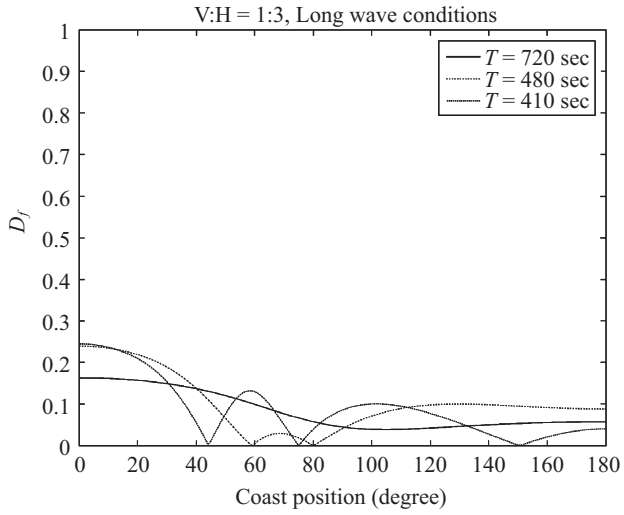

Fig. 14. The D_f around the conical island (long wave, 1:3).

long wave conditions, despite the slope of bathymetry becomes steeper. Figure 15 illustrates the dimensionless wave height around the conical island for the intermediate water waves. This figure demonstrates that the discrepancies between present solutions and those of Liu and Lin [11] are significant. The D_f around the conical island is shown in Fig. 16 and the maximal relative difference can be found for the waves with period T = 120 sec, and the magnitude is 8.7%. The D_f of others cases of this figure are all less than 1.5%. The reason for these phenomena is that the effect of the bottom slope-squared term becomes insignificant for the large conical island.

IV. CONCLUSION

Instead of the conventional MSE, which ignores the mass-conserving matching condition [15], we derived an approximate analytical solution of MMSE for an axial-symmetric conical island by adopting Hunt's direct solution of the linear dispersion relation and examined a series of calculations for different bottom slopes. Because the bottom curvature term is inherently reduced in calculations with a conical island, the slope-squared term in MMSE plays an important role in the intermediate water depth cases. As expected on the basis of previous works [9], the slope of the conical island becomes the dominant parameter resulting in the discrepancy between MMSE and MSE. The results of the present solution are in agreement with previous studies for a conical island, although the previous study, employing MSE as a governing equation, involved an analytical approach without extended terms. The curves for this kind of island are almost indistinguishable between the analytical solutions of MMSE and MSE. In the

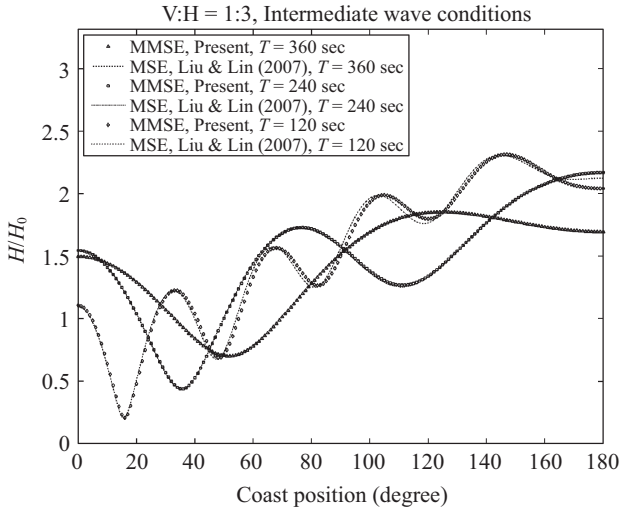

Fig. 15. The dimensionless wave height around the conical island (intermediate water wave, 1:3).

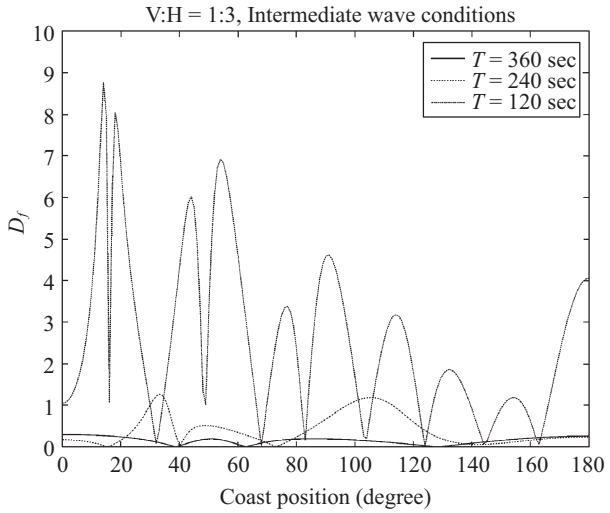

Fig. 16. The D_f around the conical island (intermediate water wave, 1:3)

intermediate water depth waves, the maximal D_f between the present solution and that of Liu and Lin [11] never exceeds 1.35%. In the calculations with steeper islands for the intermediate water waves, the maximal D_f is as high as 8.7% in the case with a slope of 1:3 and T = 120 sec. The D_f for the long-wave and critical conditions are almost less than 0.4%. Finally, we also provide evidence that the D_f increases as the coast position of the island (in degrees) decreases, i.e. toward the downstream direction.

REFERENCES

1. Berkhoff, J. C. W., "Computation of combined refraction-diffraction," *Proceeding of 13th Coastal Engineering Conference ASCE*, pp. 471-490 (1972).
2. Booij, N., "A note on the accuracy of the mild-slope equation," *Coastal Engineering*, Vol. 7, pp. 191-203 (1983).
3. Chamberlain, P. G. and Porter, D., "The modified mild-slope equation," *Journal of Fluid Mechanics*, Vol. 291, pp. 393-407 (1995).
4. Chandrasekera, C. N. and Cheung, K. F., "Extended linear refraction-diffraction model," *Journal of Waterway, Port, Coastal, and Ocean Engineering*, Vol. 123, pp. 280-286 (1997).
5. Homma, S., "On the behavior of seismic sea waves around circular island," *Geophysical Magazine*, Vol. 21, pp. 199-208 (1950).
6. Hsu, T.-W. and Wen, C.-C., "A parabolic equation extended to account for rapidly varying topography," *Coastal Engineering*, Vol. 28, pp. 1479-1498 (2001).
7. Hunt, J. N., "Direct solution of wave dispersion equation," *Journal of the Waterway Port Coastal and Ocean Division*, Vol. 105, pp. 457-459 (1979).
8. Jung, T.-H. and Suh, K.-D., "An analytic solution to the mild slope equation for waves propagating over an axi-symmetric pit," *Coastal Engineering*, Vol. 54, pp. 865-877 (2007).
9. Jung, T.-H. and Suh, K.-D., "An analytical solution to the extended mild-slope equation for long waves propagating over an axi-symmetric pit," *Wave Motion*, Vol. 45, pp. 835-845 (2008).
10. Jung, T.-H., Suh, K.-D., Lee, S. O., and Cho, Y.-S., "Linear wave reflection by trench with various shapes," *Ocean Engineering*, Vol. 35, pp. 1226-1234 (2008).
11. Liu, H.-W. and Lin, P., "An analytic solution for wave scattering by a circular cylinder mounted on a conical shoal," *Coastal Engineering Journal*, Vol. 49, pp. 393-416 (2007).
12. Liu, H.-W., Lin, P., and Shankar, N. J., "An analytical solution of the mild-slope equation for waves around a circular island on a paraboloidal shoal," *Coastal Engineering*, Vol. 51, pp. 421-437 (2004).
13. MacCamy, R. C. and Fuchs, R. A., "Wave forces on piles: A diffraction theory," *US Army Corps of Engineering, Beach Erosion Board, Technical Memorandum*, Vol. 69, Washington, DC (1954).
14. Massel, S. R., "Extended refraction-diffraction equation for surface waves," *Coastal Engineering*, Vol. 19, pp. 97-126 (1993).
15. Porter, D. and Staziker, D. J., "Extensions of the mild-slope equation," *Journal of Fluid Mechanics*, Vol. 300, pp. 367-382 (1995).
16. Suh, K.-D., Jung, T.-H., and Haller, M. C., "Long waves propagating over a circular bowl pit," *Wave Motion*, Vol. 42, pp. 143-154 (2005).
17. Yu, X.-P. and Zhang, B.-Y., "An extended analytic solution for combined refraction and diffraction of long waves over circular shoals," *Ocean Engineering*, Vol. 30, pp. 1253-1267 (2003).
18. Zhang, Y. and Zhu, S., "New solutions for the propagation of long water waves over variable depth," *Journal of Fluid Mechanics*, Vol. 278, pp. 391-406 (1994).
19. Zhu, S. and Zhang, Y., "Scattering of long waves around a circular island mounted on a conical shoal," *Wave Motion*, Vol. 23, pp. 353-362 (1996).